

## Amorphous interface layer in thin graphite films grown on the carbon face of SiC

R. Colby, M. L. Bolen, M. A. Capano, and E. A. Stach

Citation: *Appl. Phys. Lett.* **99**, 101904 (2011); doi: 10.1063/1.3635786

View online: <http://dx.doi.org/10.1063/1.3635786>

View Table of Contents: <http://apl.aip.org/resource/1/APPLAB/v99/i10>

Published by the [AIP Publishing LLC](http://www.aip.org).

---

### Additional information on *Appl. Phys. Lett.*

Journal Homepage: <http://apl.aip.org/>

Journal Information: [http://apl.aip.org/about/about\\_the\\_journal](http://apl.aip.org/about/about_the_journal)

Top downloads: [http://apl.aip.org/features/most\\_downloaded](http://apl.aip.org/features/most_downloaded)

Information for Authors: <http://apl.aip.org/authors>

## ADVERTISEMENT



**Recirculation Pumps** *with Speed Control*

Laser Cooling / Chillers  
Brushless DC • Magnetic Drive

[www.GRIpumps.com/Integrity](http://www.GRIpumps.com/Integrity)

**GRI PUMPS**  
A GORMAN-RUPP COMPANY

## Amorphous interface layer in thin graphite films grown on the carbon face of SiC

R. Colby,<sup>1,2,a)</sup> M. L. Bolen,<sup>2,3,b)</sup> M. A. Capano,<sup>2,3</sup> and E. A. Stach<sup>4</sup>

<sup>1</sup>*School of Materials Engineering, Purdue University, West Lafayette, Indiana 47907, USA*

<sup>2</sup>*Birck Nanotechnology Center, West Lafayette, Indiana 47907, USA*

<sup>3</sup>*School of Electrical and Computer Engineering, Purdue University, West Lafayette, Indiana 47907, USA*

<sup>4</sup>*Center for Functional Nanomaterials, Brookhaven National Laboratory, Upton, New York 11973, USA*

(Received 25 May 2011; accepted 18 August 2011; published online 7 September 2011)

Cross-sectional transmission electron microscopy (TEM) is used to characterize an amorphous layer observed at the interface in graphite and graphene films grown via thermal decomposition of C-face 4H-SiC. The amorphous layer does not cover the entire interface, but uniform contiguous regions span microns of cross-sectional interface. Scanning transmission electron microscopy (STEM) images and electron energy loss spectroscopy (EELS) demonstrate that the amorphous layer is a carbon-rich composition of Si/C. The amorphous layer is clearly observed in samples grown at 1600 °C for a range of growth pressures in argon, but not at 1500 °C, suggesting a temperature-dependent formation mechanism. © 2011 American Institute of Physics. [doi:10.1063/1.3635786]

The formation of epitaxial graphene and graphite by thermal decomposition of SiC has been studied for over three decades, but has seen a dramatic revitalization since the discovery of the electric-field effect in graphene in 2004.<sup>1</sup> The majority of the work based on SiC has focused on the silicon-face SiC-(0001) surface, typically in a vacuum growth environment.<sup>2,3</sup> The carbon-face SiC-(000 $\bar{1}$ ) surface has received less attention, but typically results in thin graphite films, frequently referred to as multi-layer graphene due to observations of graphene-like band structures.<sup>4-6</sup> As a result, the SiC/graphite interface is typically buried beneath several layers of graphene, and the structure is not immediately interpretable by the commonly applied surface sensitive techniques. The coupling of the first graphene layer and the C-face SiC substrate has thus far been described as both strong and weak, with a reported interface spacing varying from  $\sim 1.6$  Å– $3.2$  Å.<sup>6-8</sup> Most techniques for assessing the graphite film thickness require a model for the SiC/graphite interface, the structure of which remains likewise ambiguous and is not necessarily uniform across an entire sample.<sup>9-11</sup> Cross-sectional transmission electron microscopy (TEM) offers a more direct means of examining the film thickness and the SiC/graphite interface. The relative thicknesses of the graphite films can be determined locally, without the need for additional (often unknown) material properties, often without making assumptions as to the nature of the SiC/graphite interface. The latter benefit should become particularly apparent; this letter will report on the observation of an unexpected carbon-rich amorphous interface layer for graphite films grown on C-face 4H-SiC over a range of pressures.

Nominally on-axis 4H-SiC substrates obtained from Cree were cleaned in solvent and acid baths, then etched *in situ* with H<sub>2</sub> gas in an Epigress VP508 hot-walled reactor

to remove surface damage. The graphene and graphite thin films were formed over 10 min of thermal decomposition in vacuum (low- $10^{-5}$  mbar), or in an argon environment, at 1500 °C and 1600 °C.<sup>12</sup> Cross-sectional TEM samples were prepared using a focused ion beam (FIB) liftout method on an FEI Nova FIB/SEM, equipped with a Klöcke nanomanipulator. Protective layers of Pt/C were deposited locally in the area of interest, initially with the electron beam to avoid surface damage. TEM, scanning transmission electron microscopy (STEM), and electron energy loss spectroscopy (EELS) were obtained with an FEI Titan 80-300 operating at 300 kV, equipped with a Gatan imaging filter, with images zero-loss filtered to improve contrast. An FEI Tecnai 20 operated at 80 kV was used to check for potential electron-beam-induced effects. Cross-sections were initially left fairly thick (greater than  $\sim 100$  nm) to mitigate possible ion beam damage effects, owing to the sensitivity of graphite films.<sup>13,14</sup> While the effects of beam damage were certainly apparent, it was possible to obtain meaningful images, even for cross-sections thinned to less than 60 nm.

An amorphous layer was observed at the SiC/graphite interface in regions of all examined samples grown at 1600 °C, including samples grown at pressures of  $10^{-5}$  mbar (Fig. 1(b)), 1 mbar of Ar, and 50 mbar of Ar (Fig. 1(a)). In each region, where the amorphous layer was observed, it was locally uniform in thickness, usually persisting with no discernible variation in thickness across several microns of interface. The thickness of the amorphous layer varied from sample to sample, ranging from  $\sim 5$  to 12 Å. Graphite film thicknesses varied between samples, and by region within samples, over a range of  $\sim 4$  to 21 nm. Likewise, there was no clear correlation between amorphous layer thickness and either the graphite film thickness or growth pressure.

The amorphous layer was more clearly defined in annular dark-field (ADF) STEM images, which are conveniently bereft of the delocalization effects seen in high-resolution TEM images (Fig. 2(a)). The (0001) planes were clearly resolved in both the substrate and the graphite and just as clearly absent in the amorphous layer. Additionally,

<sup>a)</sup>Author to whom correspondence should be addressed. Electronic mail: robert.colby@pnnl.gov. Present address: Pacific Northwest National Laboratory, Richland, Washington 99354, USA.

<sup>b)</sup>Present address: National Renewable Energy Laboratory, Golden, Colorado 80401, USA.

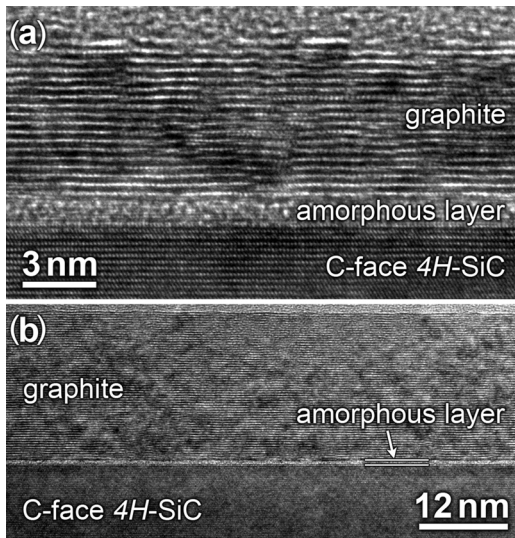


FIG. 1. (a) High resolution TEM image of a typical region of the C-face 4H-SiC and graphite film interface containing an amorphous intermediate layer, grown at 1600 °C and 50 mbar of Ar. The graphite film is  $\sim 6.8$  nm thick, while the amorphous layer is  $\sim 10$  Å (the exact thickness is obscured by delocalization of the adjacent crystalline layers). (b) TEM image of another typical region grown at 1600 °C in vacuum, with a far thicker graphite film ( $\sim 21$  nm), yet a thinner amorphous layer ( $\sim 5$  Å). The slightly mottled contrast is a product of ion and electron beam damage, especially prominent in the extremely beam-damage sensitive graphite. Both images were acquired in the SiC- $\langle 1\bar{1}00 \rangle$  direction.

ADF-STEM can be collected at higher scattering angles to obtain Z-like contrast (Fig. 2(b)). The intensity of the amorphous layer, and thus the Z-number, was in between that of the SiC substrate and the graphite film; in the absence of an unexpected contaminant, this suggested a composition of Si/C in between the SiC substrate and the pure carbon graphite. As the microscope employed was limited to annular detector

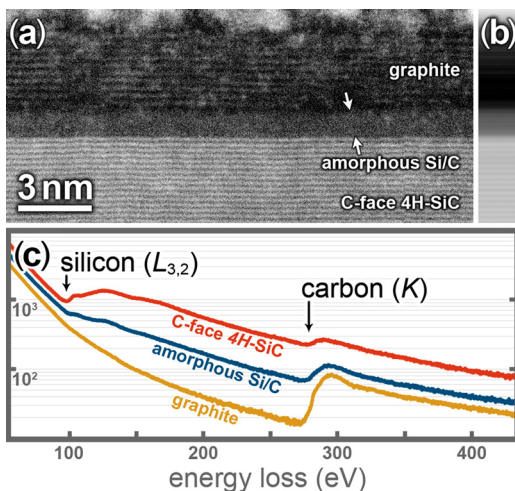


FIG. 2. (Color online) (a) ADF-STEM image of a typical region of a graphite film grown on C-face 4H-SiC at 1600 °C and 1 mbar of Ar containing an amorphous intermediate layer. Imaged from the  $\langle 1\bar{1}00 \rangle$  direction, the  $\langle 0001 \rangle$  lattice planes of both the substrate and graphite film are visible, but absent in the amorphous layer. (b) Higher angle ADF-STEM image, with Z-like contrast, averaged across  $\langle 0001 \rangle$  to reduce noise (the width of the included image is arbitrary). (c) EELS collected locally (using the STEM probe) from each of the three regions shows that the amorphous layer contains both Si and C, with a  $\sim 1:4$  of Si:C, in rough agreement with conclusions drawn from the contrast in (b). The spectra are vertically offset from each other for clarity, along a log-scale vertical axis in units of arbitrary intensity.

outer angle of  $\sim 70$  mrad, the signal obtained at angles suitable for Z-like contrast was quite low. Figure 2(b) has, therefore, been averaged along  $\langle 0001 \rangle$  to more clearly illustrate the layers' relative intensities.

EELS was utilized to more directly confirm the composition of the amorphous layer. EELS was collected with the focused STEM probe at several points along the interface from within the SiC substrate, the amorphous layer, and the graphite film. The electron beam was sufficiently localized to isolate the signals from the individual layers. As expected, both the Si-L<sub>3,2</sub> and C-K edges were apparent for the SiC substrate, while only the C-K edge emerged for the graphite film (Fig. 2(c)). The amorphous layer contained both silicon and carbon edges. No other edges were observed in any of the layers in proximity to the amorphous layer. By comparison with the nominally 1:1 stoichiometric SiC substrate, the relative Si:C ratio was found to be  $\sim 1:4$  within the amorphous layer shown in Figure 2(a), consistent with the relative intensities observed in STEM images (EELS quantification details included in supplementary information<sup>24</sup>). It is possible that the precise Si:C ratio varied from sample to sample, or even through the thickness of the amorphous layer, but the sensitivity of these samples to beam damage limited further analysis. Likewise, the energy resolution and signal to noise were insufficient to allow a more quantitative assessment of the apparent shifts and near edge structure differences for the relevant edges.

It should be specifically noted that the amorphous layer was not an artifact of sample preparation; in the very least, the formation of a silicon-containing layer above the only potential Si source (the SiC) would have been quite improbable in the top-down milling geometry used in the FIB. More direct evidence was fortuitously found in cross-sections of the wrinkles or ridges that are known to populate graphite films on C-face SiC,<sup>15–17</sup> prior to any sample preparation (Fig. 3). The amorphous Si/C layer was observed spanning the gap beneath several such locally delaminated graphite ridges. The contrast of the amorphous layer was clearly distinct from the redeposited amorphous carbon material underneath the graphite ridge (confirmed with EELS for a similar ridge). The more exposed portion of the amorphous Si/C layer beneath the ridge even appears to have suffered some ion beam damage, firmly implying that it was present prior to cross-section preparation.

Few-layer graphene films grown under similar conditions on Si-face SiC substrates were not observed to contain any such amorphous layer, in agreement with previous

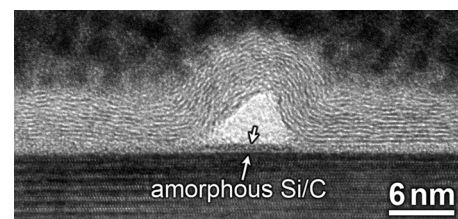


FIG. 3. Cross-sectional TEM image of one of the characteristic ridges observed in graphite grown on C-face SiC. The amorphous Si/C layer continues beneath the ridge and is distinct from the amorphous carbon material that has collected beneath the ridge as a result of sample preparation. Image acquired in the SiC- $\langle 11\bar{2}0 \rangle$  direction.

publications. Graphite films grown on C-face SiC at a lower temperature of 1500 °C could not be definitively ascribed as containing an amorphous layer either, though the interface was indistinct in many places and there did appear to be a larger spacing at the SiC/graphene interface than for the comparable Si-face samples (this latter point has been noted previously<sup>6,18,19</sup>). Therefore, some threshold for the formation of the amorphous layer seems to have existed, being either dependent upon temperature or temperature-related processing conditions. As there are more than twice as many carbon atoms in graphite (by volume) than in 4H-SiC, a carbon-rich layer of Si/C could have accumulated prior to the formation of a stable graphene sheet. At sufficient temperatures, the SiC decomposition rate during growth might have outpaced the rate at which the resulting silicon could migrate or diffuse to a free surface. The kinetics of growth on C-face SiC, in particular after the surface is covered in graphite, are not yet well enough understood to postulate a more precise mechanism. The amorphous layer was also reminiscent of the intergranular films observed in liquid-phase sintered SiC in the presence of residual additives or contaminants.<sup>20,21</sup> The excess carbon near the SiC/graphite interface could have served as an analogous “contamination,” with the resulting amorphous layer mitigating the expected interfacial strain; the in-plane lattice mismatch between graphite and SiC is ~20% at room temperature, and in-plane thermal expansion mismatch ~60% to 80%.<sup>16,22,23</sup> It is possible that the formation of amorphous layer is governed both by the conditions during growth and sample cool-down.

To summarize, an amorphous Si/C layer has been observed at the interface between C-face 4H-SiC and graphite films grown by thermal decomposition at 1600 °C, from vacuum to 50 mbar of Ar. The layer was frequently observed across microns of cross-sectional interface by TEM, with each contiguous segment fairly uniform in thickness. There were variations between regions and samples with no clear correlation to growth pressure or the overlaying graphite film thickness, though there seems to have been a growth temperature-related threshold for its emergence. EELS confirmed that the layer was a carbon-rich ~Si<sub>1</sub>/C<sub>4</sub>. Without a larger-scale means of detecting the amorphous layer under the surface, it has not been possible to investigate the potential consequences of the amorphous layer: but such effects

might be expected, for instance, on the mobility of the graphene or graphite films, and therefore on any devices fabricated on such films.

M.L.B. and M.A.C. acknowledge support from DARPA, the Air Force Research Laboratory, and Group 4 Development, LLC, and E.A.S. acknowledges support from the U.S. Department of Energy, Office of Basic Energy Sciences, under Contract No. DE-AC02-98CH10886.

<sup>1</sup>K. Novoselov, *Science* **306**, 666 (2004).

<sup>2</sup>P. First, W. Heer, T. Seyller, C. Berger, J. Stroscio, and J. Moon, *MRS Bull.* **35**, 296 (2010).

<sup>3</sup>C. Berger, Z. Song, T. Li, X. Li, A. Ogbazghi, R. Feng, Z. Dai, A. Marchenkov, E. Conrad, and N. Phillip, *J. Phys. Chem. B* **108**, 19912 (2004).

<sup>4</sup>J. Hass, W. de Heer, and E. Conrad, *J. Phys. Condens. Matter* **20**, 323202 (2008).

<sup>5</sup>F. Varchon, P. Mallet, L. Magaud, and J. Veuillen, *Phys. Rev. B* **77**, 165415 (2008).

<sup>6</sup>J. Borysiuk, K. Grodecki, A. Wyszomolek, W. Strupinski, R. Stepniewski, and J. Baranowski, *J. Appl. Phys.* **108**, 013518 (2010).

<sup>7</sup>I. Forbeaux, J. Themlin, and J. Debever, *Surf. Sci.* **442**, 9 (1999).

<sup>8</sup>J. Hass, R. Feng, J. Millan-Otoya, X. Li, M. Sprinkle, P. First, W. de Heer, E. Conrad, and C. Berger, *Phys. Rev. B* **75**, 214109 (2007).

<sup>9</sup>L. Muehlhoff, M. Bozack, W. Choyke, and J. Yates, *J. Appl. Phys.* **60**, 2558 (1986).

<sup>10</sup>J. Veuillen, F. Hiebel, L. Magaud, P. Mallet, and F. Varchon, *J. Phys. D: Appl. Phys.* **43**, 374008 (2010).

<sup>11</sup>A. Drabińska, K. Grodecki, W. Strupiński, R. Bożek, K. Korona, A. Wyszomolek, R. Stepniewski, and J. Baranowski, *Phys. Rev. B* **81**, 245410 (2010).

<sup>12</sup>M. Bolen, S. Harrison, L. Biedermann, and M. Capano, *Phys. Rev. B* **80**, 115433 (2009).

<sup>13</sup>A. Krashennnikov and F. Banhart, *Nature Mater.* **6**, 723 (2007).

<sup>14</sup>D. Teweldebrhan and A. Balandin, *Appl. Phys. Lett.* **94**, 013101 (2009).

<sup>15</sup>Luxmi, P. Fisher, N. Srivastava, R. Feenstra, Y. Sun, J. Kedzierski, P. Healey, and G. Gu, *Appl. Phys. Lett.* **95**, 073101-3 (2009).

<sup>16</sup>L. Biedermann, M. Bolen, M. Capano, D. Zemlyanov, and R. Reifenger, *Phys. Rev. B* **79**, 125411 (2009).

<sup>17</sup>S. Harrison, M. Capano, and R. Reifenger, *Appl. Phys. Lett.* **96**, 081905 (2010).

<sup>18</sup>J. Borysiuk, W. Strupinski, A. Wyszomolek, K. Grodecki, R. Stepniewski, and J. Baranowski, *J. Appl. Phys.* **105**, 023503-5 (2009).

<sup>19</sup>X. Weng, J. Robinson, K. Trumbull, R. Cavalero, M. Fanton, and D. Snyder, *Appl. Phys. Lett.* **97**, 201905 (2010).

<sup>20</sup>H. Kleebe, *J. Eur. Ceram. Soc.* **10**, 151 (1992).

<sup>21</sup>E. Volz, A. Roosen, S. Wang, and W. Wei, *J. Mater. Sci.* **39**, 4095 (2004).

<sup>22</sup>Z. Li and R. Bradt, *J. Am. Ceram. Soc.* **69**, 863 (1986).

<sup>23</sup>D. Tsang, B. Marsden, S. Fok, and G. Hall, *Carbon* **43**, 2902 (2005).

<sup>24</sup>See supplementary material at <http://dx.doi.org/10.1063/1.3635786> for more details as to the quantification of EELS data.